HIV-1 Vaccine Development: Constrained Peptide Immunogens Show Improved Binding to the Anti-HIV-1 gp41 MAb

G. B. McGaughey,*,‡ M. Citron,§ R. C. Danzeisen,|| R. M. Freidinger,⊥ V. M. Garsky,⊥ W. M. Hurni,# J. G. Joyce,# X. Liang,§ M. Miller,|| J. Shiver,§ and M. J. Bogusky*,⊥

Departments of Molecular Systems, Medicinal Chemistry, Virus and Cell Biology, Viral Vaccine Research, and Biological Chemistry, Merck Research Laboratories, P.O. Box 4, West Point, Pennsylvania 19486

Received October 4, 2002; Revised Manuscript Received December 20, 2002

ABSTRACT: The human immunodeficiency virus type I (HIV-1) transmembrane glycoprotein gp41 mediates viral entry through fusion of the target cellular and viral membranes. A segment of gp41 containing the sequence Glu-Leu-Asp-Lys-Trp-Ala has previously been identified as the epitope of the HIV-1 neutralizing human monoclonal antibody 2F5 (MAb 2F5). The 2F5 epitope is highly conserved among HIV-1 envelope glycoproteins. Antibodies directed at the 2F5 epitope have neutralizing effects on a broad range of laboratory-adapted HIV-1 variants and primary isolates. Recently, a crystal structure of the epitope bound to the Fab fragment of MAb 2F5 has shown that the 2F5 peptide adopts a β-turn conformation [Pai, E. F., Klein, M. H., Chong, P., and Pedyczak, A. (2000) World Intellectual Property Organization Patent WO-00/61618]. We have designed cyclic peptides to adopt β-turn conformations by the incorporation of a side-chain to side-chain lactam bridge between the i and $i + 4$ residues containing the Asp-Lys-Trp segment. Synthesis of extended, nonconstrained peptides encompassing the 2F5 epitope revealed that the 13 amino acid sequence, Glu-Leu-Leu-Glu-Leu-Asp-Lys-Trp-Ala-Ser-Leu-Trp-Asn, maximized MAb 2F5 binding. Constrained analogues of this sequence were explored to optimize 2F5 binding affinity. The solution conformations of the constrained peptides have been characterized by NMR spectroscopy and molecular modeling techniques. The results presented here demonstrate that both inclusion of the lactam constraint and extension of the 2F5 segment are necessary to elicit optimal antibody binding activity. The ability of these peptide immunogens to stimulate a high titer, peptide-specific immune response incapable of viral neutralization is discussed in regard to developing an HIV-1 vaccine designed to elicit a 2F5-like immune response.

The human immunodeficiency virus type I (HIV-1) envelope glycoprotein is synthesized as the precursor gp160, which is proteolytically cleaved into two noncovalently associated protein subunits, a surface subunit (gp120), and a transmembrane subunit (gp41) (Figure 1) (*2*−*4*). The gp120 envelope protein is responsible for binding to the CD4 cell-surface receptor and a chemokine co-receptor, CCR5 or CXCR4 (*5*−*7*). Following receptor binding, the membrane-anchored gp41 mediates fusion of the viral and target cell membranes. The gp41 ectodomain contains a hydrophobic, glycine-rich fusion peptide (amino acids 512−527) at the amino terminus, which is essential for membrane fusion (numbering based on HXB2 gp160 variant as described in ref *8*). Two 4,3 hydrophobic repeat regions following the fusion peptide are defined by a heptad repeat $(abcdefg)_n$, where the residues occupying the a and d positions are predominantly hydrophobic. The two heptad repeat regions are referred to as the N36 (residues 546−581) and C34 (residues 628−661) peptides. A loop region containing a disulfide linkage separates the two heptad repeat regions. Following the second heptad repeat is the 2F5 epitope (amino acids 662−667), a six residue sequence recognized by MAb 2F5 (*9*, *10*). The region of the gp41 ectodomain proximal to the viral membrane is abundant in the amino acid tryptophan and has been shown to be critical for the membrane fusion mechanism of HIV-1 (*11*−*13*) (Figure 1).

gp41 exists in two distinct conformations, a native or nonfusogenic state and a fusion-active state (*14*). On the surface of free virions, gp41 exists with the N-terminal fusion peptide inaccessible in the native state. Following interaction of the gp120/gp41 complex with cell-surface receptors, gp41 undergoes a series of conformational changes leading to the fusion-active conformation (*14*). These conformational changes expose the fusion peptide, which inserts into the target membrane bringing the viral and target membranes into proximity allowing viral entry into the target cell (*14*).

Crystallographic analysis has demonstrated that the gp41 fusion-active core adopts a six-stranded helical bundle (*8*). Three N-terminal peptides adopt a homo-trimeric helical coiled−coil forming the center of the bundle. Three C-terminal peptide helices pack into hydrophobic grooves on the outer surface of the N-peptide core in an antiparallel

* Corresponding authors. (G.B.M.) Tel.: (215) 652-7183. Fax: (215) 652-4625. E-mail: georgia_mcgaughey@merck.com. (M.J.B.) Tel.: (215) 652-3801. Fax: (215) 652-4674. E-mail: michael_bogusky@merck.com.

‡ Department of Molecular Systems.

§ Department of Viral Vaccine Research.

|| Department of Biological Chemistry.

⊥ Department of Medicinal Chemistry.

Department of Virus and Cell Biology.

10.1021/bi026952u CCC: $25.00
Published on Web 02/27/2003

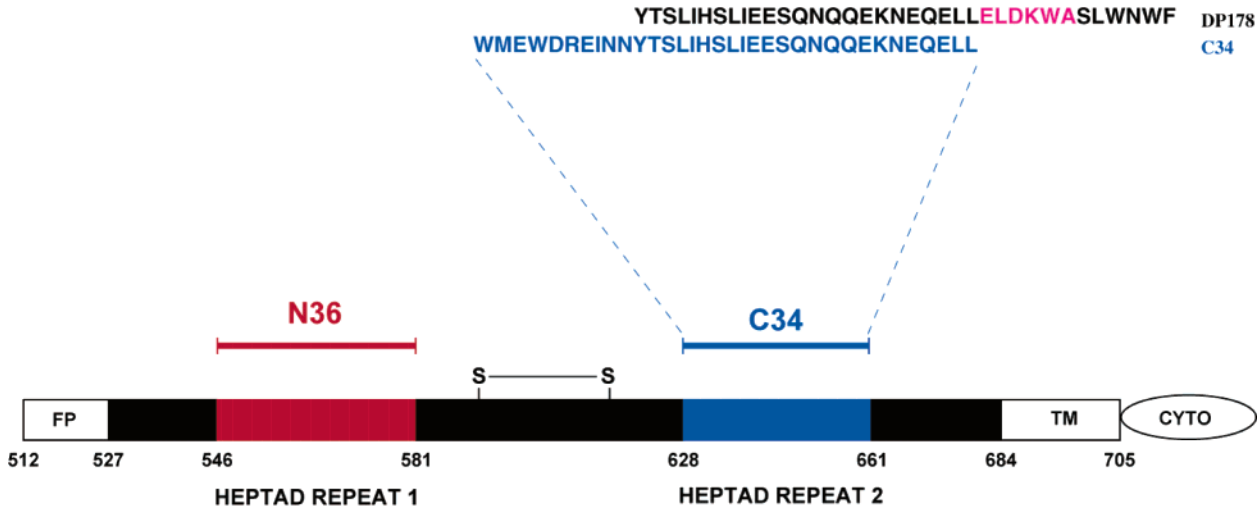

FIGURE 1: Schematic diagram of HIV-1 gp41 (adapted from ref *8*). The important functional regions of the gp41 envelope glycoprotein including the fusion peptide (fp), the two heptad repeats (N36 and C34), the region spanning the 2F5 epitope (residues 661−684), the transmembrane region (tm), and the cytoplasmic domain (cyto) are indicated. The residues are numbered based on the HXB2 gp160 variant as described in ref *8*.

manner forming a trimer-of-hairpins structure. The trimer-of-hairpins likely resembles the fusion-active conformation since this structural motif brings the N-terminal region of gp41 containing the fusion peptide together with the C-terminal region that is anchored to the viral membrane (*14*, *15*). This conformational rearrangement brings the viral and target cell membranes together, promoting fusion.

Two classes of synthetic linear peptides derived from the gp41 ectodomain have been shown to inhibit viral fusion (*16*−*18*). The sequences of these peptides overlap with either the N- or the C-terminal heptad repeat domains. These peptides are thought to inhibit infection by binding to gp41 and prevent the conformational changes that result in the fusion-active state. One peptide currently in clinical trials (DP178) is derived from the C-terminal region of gp41 (residues 638−673) and successfully blocks viral membrane fusion in vitro thereby validating the inhibition of the gp41 fusogenic state as a viable drug target (*16*, *19*, *20*). Although DP178 is effective in the treatment of HIV-1 infection, the 36-residue peptide lacks many of the desirable qualities of useful pharmaceutical agents such as oral bioavailability (*21*). Inhibiting viral fusion provides a potential therapeutic strategy for the development of small, synthetic, orally bioavailable molecules; however, a more globally accessible and cost-effective therapy would come in the form of an HIV-1 vaccine (*22*).

A prerequisite for an HIV-1 vaccine is an immunogen capable of eliciting a broadly neutralizing antibody and/or cell-mediated immune response (*22*, *23*). Several broadly neutralizing HIV-1 monoclonal antibodies (MAb) have been characterized: 4E10 (*24*), Z13 (*25*), and 2F5 (*9*, *10*), which bind to gp41; and 1b12 (*26*), 2G12 (*27*), and X5 (*28*), which bind to gp120. The identification of MAb 2F5 that neutralized both cell culture-adapted HIV-1 variants and primary clinical isolates served to identify a highly conserved neutralizing epitope shared by many strains (*9*, *10*). Amino acid sequences recognized by MAb 2F5 were identified from a phage display library expressing random hexapeptides (*9*). The results suggested that the MAb epitope is comprised of the amino acid sequence Glu-Leu-Asp-Lys-Trp-Ala with Asp-Lys-Trp forming the core sequence (*10*). This sequence corresponding to residues 662−667 of the gp41 ectodomain is conserved in 72% of otherwise highly variable HIV-1 isolates (*9*).

Recently, a patent application was published that depicted the complexed crystal structure of the 2F5 epitope in a β-turn conformation bound to the Fab fragment of MAb 2F5 (*1*). We have expanded upon the known crystal structure by combining traditional structure−activity relationships, NMR, and molecular modeling techniques to elucidate the structural components required for optimal antibody recognition (*1*, *29*).

MATERIALS AND METHODS

Peptide Synthesis. Peptides were synthesized using standard Merrifield solid-phase methodologies (*30*). Formation of the intramolecular side-chain to side-chain lactam bridge was achieved while the peptide was on the solid support (*31*). Air oxidation at pH 7.5 was the method of choice for the formation of the Cys to Cys disulfide bridged compound **1**. The peptide structures were characterized by high-resolution mass spectrometry and NMR.

MAb 2F5 Reactivity Assay. A competitive solution binding assay was designed to assess and rank the peptides' binding affinity to the broadly neutralizing monoclonal antibody 2F5. In the assay, the peptide of interest competes with a fixed and limiting amount of a labeled reference peptide (biotin-DP178) for a limiting amount of MAb 2F5 bound to plastic. Nunc F8 MAXISORP 8 well strips were coated with MAb 2F5 at 20 ng/well in phosphate-buffered saline (PBS, 6.25 mM sodium phosphate, pH 7.2, 0.15 M NaCl) and over-coated with 1% BSA in PBS containing 0.1% sodium azide. The reference peptide (biotin-DP178) was biotin-labeled by reaction of Ac-Cys-DP178-NH_2 with PEO-maleimide-activated biotin (Pierce, Rockford, IL) and purified by gel filtration chromatography. The reference peptide was used at a concentration of 8×10^{-14} mol/well. Test samples were dissolved at a nominal concentration of 1 mg/mL (w/v) in an appropriate solvent and diluted 500-fold in assay diluent (1% BSA in PBS containing 0.1% Tween 20 and 0.1% sodium azide) as the top point for a 3-fold, 7-point dilution

series. An equal volume of test sample and biotin-DP178 (125 μL of each) were mixed in a tube, and 200 μL was added to a well precoated with MAb 2F5. After an overnight incubation at ambient temperature the wells were washed with diluent, and detection of bound biotin-DP178 was accomplished with horseradish peroxidase-coupled streptavidin utilizing 3,3′,5,5′-tetramethylbenzidine substrate. The concentration of sample peptide required to reduce the signal from the labeled reference peptide to 50% of the maximum bound control was used to calculate the number of moles of sample peptide required to compete off 1 mol of labeled reference peptide.

Preparation of Peptide Conjugates. Peptides used for conjugation were synthesized with a Cys residue on either the amino or the carboxy terminus for covalent coupling to a maleimide-activated carrier protein. For this study, the carrier protein used was the outer membrane protein complex (OMPC)[1] of *Neisseria meningitidis* whose purification and properties have been described elsewhere (*32*, *33*). Peptide stocks were prepared in HEPES-EDTA buffer (100 mM HEPES, 2 mM EDTA, pH 7.3) at 1 mg/mL, and the thiol concentration was determined by Ellman's procedure using 5,5′-dithionitrobenzoic acid (DTNB) (*34*). OMPC was derivatized with sulfosuccinimidyl 4-(*N*-maleimidomethyl)-cyclohexane-1-carboxylate, sSMCC (Pierce, Rockford, IL) to introduce a thiol-reactive maleimide group. Briefly, OMPC was buffered to 20 mM HEPES, pH 7.3, and sSMCC was added at a 10-fold molar excess over the total Lys content. The reaction was carried out for 4−5 h at 4 °C in the dark after which excess reagent was removed by exhaustive dialysis against HEPES-EDTA buffer. The maleimide content of the derivatized OMPC was determined by quantitation of thiol consumption. Conjugates were prepared by mixing peptide and activated OMPC at a 1:1 thiol/maleimide ratio in HEPES-EDTA buffer. A control of activated OMPC alone was carried through the procedure. Reactions were carried out for 16−20 h at 4 °C in the dark. Residual reactive maleimide groups were quenched by addition of 2-mercaptoethanol to 15 mM and incubated at 4 °C for 2−4 h. To remove residual free peptide and reagents, controls and conjugates were exhaustively dialyzed against HBS (20 mM HEPES, 0.15 M NaCl, pH 7.3). Protein concentration was determined by a modified Lowry assay (*35*), and peptide incorporation was determined by a quantitative amino acid analysis comparison of conjugate and control as previously described (*36*).

HIV-1 Neutralization Assay. HIV-1 infection was measured in a single-cycle infectivity assay based on p4-2 cells (*37*), a gift of Ned Landau (The Salk Institute). HIV-1 infection of these cells results in production of the viral protein Tat, which transactivates the integrated β-galactosidase gene in the p4-2 cells and can be detected with a chemiluminescent substrate. Cells were maintained at 37 °C/5% CO_2 in phenol red-free DMEM (CellGro) containing 10% FBS (Hyclone) and 0.5 μg/mL puromycin (Clontech). The day before infection, cells were removed from stock flasks with trypsin-EDTA (LifeTechnologies), seeded in white 96-well Costar 3894 plates (Costar) at 2500 cells/well, and incubated overnight. The HIV-1 viral stock (HXB2 strain, Advanced Biotechnology, Inc.) was diluted to a concentration predetermined to yield a signal in the linear range of the assay (final moi $\approx$ 0.02). The viral stock was incubated for 10 min at room temperature with dilutions of heat-inactivated Guinea pig sera and added to cells from which the media had been removed. Cells and virus were incubated an additional 48 h to allow a single round of infection to occur. β-galactosidase production was measured using a GalScreen chemiluminescent detection kit according to the manufacturer's instructions and a Dynex luminometer. This assay is sensitive to known HIV-1-neutralizing antibodies such as IgG1b12 and 2F5, which typically blocks HXB2 infectivity with IC_{50} values of 50−100 ng/mL (data not shown). Neutralization titers are expressed as the reciprocal of the lowest dilution inhibiting 50% of the infectivity.

Animal Immunizations. Six to 10 week-old female guinea pigs were obtained from Harlan Inc., Indianapolis, IN and maintained in the animal facilities of Merck Research Laboratories in accordance with institutional guidelines. All animal experiments were approved by Merck Research Laboratories Institutional Animal Care and Use Committee (IACUC). Antigens were prepared in phosphate-buffered saline at concentrations of 250 μg/mL. The saponin-based QS21 adjuvant was added to the peptide solutions immediately prior to immunization at a final concentration of 100 μg/mL. Guinea pigs were immunized with 400 μL of an antigen injected into the quadriceps of the animal. The immunizations were given three times at 4-week intervals. Blood samples were collected at three weeks following each injection and stored at 4 °C prior to antibody titer determinations.

Enzyme-Linked Immunosorbent Assay (ELISA). Streptavidin-coated 96-well plates (Pierce, Rockford, IL) were coated with 0.2 μg of a biotinylated peptide in 50 μL of bicarbonate buffer, pH 9.6, per well at 4 °C overnight. Plates were washed with PBS containing 0.05% Tween-20 (PBST) and blocked with 3% skim milk in PBST (milk-PBST). Serial 1:4 dilutions of testing samples were prepared in Milk-PBST. A total of 100 μL of the diluted sample was added to each well of the antigen-coated plates, and the plates were incubated at 24 °C for 1 h. Following three washes with PBST, the plates were incubated with HRP-conjugated goat anti-guinea pig IgG (Zymed, San Francisco, CA). This was followed by three washes and the addition of 100 μL of 1 mg/mL *o*-phenylenediamine dihydrochloride substrate (Sigma, St. Louis, MO) per well. Plates were read at 490 nm 30 min later using a microplate reader (Molecular Devices, Sunnyvale, CA). The antibody titers were calculated as reciprocals of the highest dilutions, which gave optical density values above two standard deviations of the mean of the secondary antibody conjugate control.

NMR Spectroscopy. Synthetic peptide samples were dissolved in either PBS (6.25 mM sodium phosphate, 0.15 M NaCl, pH 7.2) or DMSO-d_6 at concentrations ranging

[1] Abbreviations: HEPES, *N*-[2-hydroxyethyl]piperazine-*N*′-[2-ethanesulfonic acid]; sSMCC, sulfosuccinimidyl 4-(*N*-maleimidomethyl)-cyclohexane-1-carboxylate; OMPC, outer membrane protein complex; HBS, HEPES-buffered saline; DTNB, 5,5′-dithionitrobenzoic acid; OMPC, outer membrane protein complex of *Neisseria meningitidis;* moi, multiplicity of infection; TMS, tetramethylsilane; TSP, 3-(trimethylsilyl)propionate-2,2,3,3-d_4; PBS, phosphate-buffered saline; DMSO-d_6, deuterated dimethyl sulfoxide; TOCSY, total correlation spectroscopy; ROESY, rotating frame Overhauser enhancement spectroscopy; RMSD, root-mean-square deviation; Dap, L-α-diaminopropionic acid; GA, genetic algorithm; DG, distance geometry; Aha, 6-aminohexanoic acid.

between 1 and 2 mM. NMR spectra were recorded on a Varian Inova 600 MHz spectrometer at 25 °C. Proton chemical shifts were referenced to tetramethylsilane (TMS) in DMSO-d_6 solution or sodium 3-(trimethylsilyl)propionate-2,2,3,3-d_4 (TSP) in PBS solution at 0.00 ppm. The water resonance in PBS solution was suppressed by selective saturation using an attenuated transmitter pulse during the recycle delay. Sequential ^{1}H resonance assignments were made with two-dimensional TOCSY (*38*, *39*) and ROESY (*40*, *41*) spectra using standard methodologies. TOCSY and ROESY spectra were acquired in the phase-sensitive mode using the hypercomplex method. TOCSY spectra were recorded with 1K complex points in t_2 and 512 points in t_1. Spin locking in the TOCSY experiments was achieved with an MLEV-17 (*42*) mixing sequence for a duration of 50−65 ms preceded by a 2.0-ms trim pulse. After zero-filling to 2K in the second dimension, the two-dimensional data matrixes were multiplied by a Gaussian window function and Fourier transformed. ROESY spectra were acquired using a mixing time of 100 ms with a spin-lock radio frequency (Rf) field strength of ∼3.8 kHz. The experimental parameters, including the mixing time and the Rf field strength of the mixing pulse were optimized to minimize TOCSY artifacts in the spectra. Spin-locking was achieved by the application of a series of 30° pulses with a hard 90° pulse on each side of the spin-lock to compensate for off-resonance effects (*43*, *44*). 1K complex points were acquired in t_2 and 512 increments were collected in t_1. After zero-filling to 2K in the second dimension, the two-dimensional data matrixes were multiplied by a Gaussian window function and Fourier transformed. Distance constraints for structural calculations were derived from ROE cross-peak intensities by volume integration of the cross-peaks using the VNMR (Varian, Inc.) mark routine. Interproton distances were estimated from ROE cross-peak intensities using either a geminal methylene pair or an ortho aromatic pair as fixed internal reference distances of 1.8 or 2.5 Å, respectively. Estimated interproton distances were derived using the isolated spin-pair approximation (*44*), $r_{ij} = r_{ref}\ (a_{ref}/a_{ij})^{1/6}$ where r_{ij} is the estimated interproton distance, r_{ref} is the fixed internal reference distance, and a_{ref} and a_{ij} are the ROE cross-peak intensities of the reference and estimated cross-peaks, respectively. The approximate interproton distances were tabulated and grouped into distance boundaries corresponding to 1.8−2.8 Å (strong), 1.8−3.5 Å (medium), and 1.8−5.0 Å (weak) for structural calculations. For all nonstereospecifically assigned geminal methylene protons, a 0.5-Å pseudoatom correction was added to the distance boundary.

The temperature dependence of amide proton chemical shifts was examined by recording one-dimensional ^{1}H spectra in DMSO-d_6 over a temperature range of 25−55 °C in 10° increments. The temperature coefficients were calculated to determine the relative solvent accessibility of the amide hydrogens. The chemical shifts varied linearly with temperature in all cases indicating that no significant conformational changes were occurring over the temperature range indicated.

Computational Chemistry. A modified distance geometry approach has been developed to address the inherent flexibility of small cyclic peptides and the frequently occurring circumstance where the entire set of experimental distance constraints are not consistent with a single conformation (*46*). A genetic algorithm (GA) is used to optimize the number of experimental NOE (ROE) constraints incorporated into the conformation-generation cycle in cases where a subset of the distance constraints are not satisfied. The GA option is only used in cases where the distance geometry methodology was unable to produce a conformation consistent with all measured experimental constraints (ROE-derived distance restraints, vicinal proton−proton coupling constants ($^3J_{HN\alpha}$) and intramolecular hydrogen-bonds). This method is able to produce conformations consistent with a subset of experimental constraints.

The GA was used to generate 40 conformations from the experimentally derived constraints. Methylene protons were not stereospecifically assigned and were allowed to chirally interconvert during the computation. The resultant conformers were individually examined, and all ROE violations were identified. When appropriate, torsional angle (ϕ) and/or intramolecular hydrogen bond constraints were incorporated in some structural calculations.

Resulting conformations containing the fewest number of ROE-derived distance boundary violations were retained and visually inspected for the presence of a cation/π-stacking interaction (*47*) between the Trp and the Lys side chains. The observed cation/π-stacking interaction is consistent with experimentally observed upfield-shifted (ring current-shifted) Lys side-chain resonances.

The best structure determined by the aforementioned methodology was used as the starting structure for standard distance geometry calculations. The final GA structure and the GA-satisfied distance constraints were incorporated into the metric matrix distance geometry algorithm JIGGLE to generate an ensemble of 100 conformations (*46*). Hydrogen bond and torsional angle constraints were not included in the calculations. The projected conformations were subjected to energy minimization using the MMFFs force field (*48*) and a square-well potential with a restraint constant of 240 kcal/(mol Å^2). Energy minimizations were performed using a distance-dependent dielectric of 2 with the ROE-derived distance restraints applied during minimization. Structures with energies exceeding 20 kcal/mol above the global minimum energy conformation were discarded. The conformations were analyzed to determine their secondary structure.

RESULTS

Peptide Structure−Activity Relationships. Structures **1**−**2** (Table 1) were claimed in the patent application (*1*) as examples of constrained cyclic peptides adopting a β-turn conformation that is recognized by the monoclonal antibody 2F5. The peptides presented in the patent, and in addition, the N-acetylated form of **2** (structure **3**) demonstrated poor affinity in a competitive solution-based antibody-binding assay performed in our laboratory (*49*) (the reported reactivity values are relative binding strengths (relative to DP178 in competition ELISA) and not intrinsic antibody affinities; throughout the text the term affinity reflects relative binding strengths). However, two important structural details were revealed following the synthesis of the peptides from the patent. Structure **1**, which contains a disulfide bridge between Cys residues *i* and *i* + 4, is highly flexible and does not adopt a preferred conformation in solution. The incorporation of an *i* to *i* + 4 lactam bridge between the L-α-diaminopropionic acid (Dap) and the Glu side chains

Table 1: Peptide Sequence, Secondary Structure, and Relative MAb 2F5 Binding Affinity of the gp41 Immunogen Constructs[a]

Structure	Structure Sequence	Secondary Structure	Reactivity
1	H-Glu-Cys-Asp-Lys-Trp-Cys-Ser-OH	Disordered	>191,400
2	H-Glu-Dap-Asp-Lys-Trp-Glu-Ser-OH	Type I β-turn	158,400
3	Ac-Glu-Dap-Asp-Lys-Trp-Glu-Ser-OH	Type I β-turn	92,400
4	Ac-Glu-Dap-Asp-Lys-Trp-Asp-Ser-OH	Type I β-turn	25,800
5	Ac-Glu-Glu-Asp-Lys-Trp-Dap-Ser-OH	Type I β-turn (non ideal)	>113,750
6	Ac-Glu-Leu-Leu-Glu-Dap-Asp-Lys-Trp-Asp-Ser-Leu-Trp-Asn-OH	Type I β-turn	1.1
7	Glu-Dap-Asp-Lys-Trp-Glu-Ser	Disordered*	>191,400
8	Ac-Glu-Leu-Leu-Glu-Leu-Asp-Lys-Trp-Ala-Ser-Leu-Trp-Asn-NH_2[#]	Disordered*	120
9	Ac-Glu-Leu-Leu-Glu-Dap-Asp-Lys-Trp-Asp-Ser-OH	Type I β-turn*	730
10	Ac-Glu-Dap-Asp-Lys-Trp-Asp-Ser-Leu-Trp-Asn-OH	Type I β-turn*	225
11	Ac-Glu-Leu-Leu-Glu-Dap-Asp-Lys-Trp-Asp-Ser-Leu-Trp-Asn-Aha-Cys-NH_2	Type I β-turn	1.1
12	Ac-Cys-Aha-Glu-Leu-Leu-Glu-Dap-Asp-Lys-Trp-Asp-Ser-Leu-Trp-Asn-NH_2	Type I β-turn*	1.9

[a] Structures **1**−**6** and **11** were calculated using the distance geometry algorithm described in Materials and Methods with the incorporation of NMR-derived distance constraints. All structures were determined on samples dissolved in PBS solution with the exception of structures **1** and **5**, which were determined on samples dissolved in a DMSO-d_6 solution. A solution-based ELISA assay was used to measure the relative affinities of the peptides bound to MAb 2F5. *The secondary structures of **7**−**10** and **12** were qualitatively assessed by the analysis of backbone ROEs and vicinal coupling constants. Qualitative analysis of ROESY spectra allows the identification of specific patterns of ROE interactions that are indicative of particular secondary structures. Specifically, the ROE observable distances that permit the identification of β-turn types include the sequential $d_{\alpha N}(2,3)$, $d_{NN}(2,3)$, and $d_{NN}(3,4)$ distances where the numbering refers to the position of the amino acid within the turn. Types I and II reverse turns may be distinguished by the relative intensities of the $d_{\alpha N}(2,3)$, $d_{NN}(2,3)$, and $d_{NN}(3,4)$ ROE cross-peaks. A type I β-turn is characterized by a medium $d_{\alpha N}(2,3)$ cross-peak intensity and strong $d_{NN}(2,3)$ and $d_{NN}(3,4)$ cross-peak intensities corresponding to interproton distances of 3.4, 2.6, and 2.4 Å, respectively. A type II β-turn will display strong $d_{\alpha N}(2,3)$ and $d_{NN}(3,4)$ cross-peak intensities and a weak or nonexistent $d_{NN}(2,3)$ cross-peak intensity corresponding to distances of 2.2, 2.4, and 4.5 Å, respectively. The above analysis assumes that an ideal type I or type II β-turn is present. Deviations from ideality (distorted or nonideal reverse turns) or distortions in the relative ROE intensities because of molecular motions may compromise the distinctions between the various turn types. Vicinal amide proton to C_α proton coupling constants ($^3J_{HN\alpha}$) are also useful in the delineation of turn types. A type I turn displays $^3J_{HN\alpha}$ values of ∼4 and ∼9 Hz (ϕ_2 −60°, ϕ_3 −90°), and a type II turn displays $^3J_{HN\alpha}$ values of ∼4 and ∼5 Hz (ϕ_2 −60°, ϕ_3 +90°) for residues 2 and 3 of the turn. Disordered (random coil) structures are identified by an overall paucity of ROEs, moderate intensity sequential $d_{\alpha N}$ ROEs, and averaged (∼7 Hz) backbone vicinal coupling constants. [#] The free amino and carboxy analogue (Glu-Leu-Leu-Glu-Leu-Asp-Lys-Trp-Ala-Ser-Leu-Trp-Asn) has been characterized in detail by NMR (*29*). A subpopulation of structures was identified where the Asp-Lys-Trp segment adopts a backbone conformation similar to the 2F5-bound β-turn structure previously determined by X-ray (*1*). In a substantial population of conformers, the turn was accompanied by an upstream α-helix and/or a downstream extended structure.

stabilizes peptides **2** and **3** into a defined type I β-turn conformation in solution. Synthesis of the N-acetylated analogue of **2** (structure **3**) resulted in a nearly 2-fold enhancement in MAb 2F5 binding affinity. Since N-blocked peptides are less susceptible to proteolytic cleavage and there was no loss in affinity, the *N*-acetyl capping group was maintained in subsequently synthesized peptides (Table 1).

Three structural features were examined in detail to explore their effects on MAb 2F5 affinity: (1) the importance of the lactam bridge between the *i* and *i* + 4 residues within the epitope, (2) the effect of amino acid substitutions within the 2F5 epitope, and (3) the effect of extending the 2F5 epitope segment (Glu-Leu-Asp-Lys-Trp-Ala) in both the N- and the C-terminal directions. Although appreciable enhancement of antibody affinity was not observed with structures **2** and **3** when compared to structure **1**, it was evident that the secondary structure in solution is highly dependent on the nature of the constraint used. Incorporation of the *i* to *i* + 4 lactam bridge stabilized structures **2** and **3** into defined type I β-turn conformations consistent with the antibody-bound epitope conformation. The *i* to *i* + 4 lactam bridge as well as the chemical nature of the constraint are both important in stabilization of the reverse turn conformation. Furthermore, reversing the directionality of the lactam amide bond with a concomitant shift in its position by interchanging the Glu and Dap residues alters the β-turn conformation resulting in a significant reduction of 2F5 MAb affinity (compare **5** relative to **3**). The acyclic analogue of **2** was synthesized to examine the effects of removing the lactam constraint on secondary structure and antibody affinity. The nonconstrained peptide analogue, **7**, was disordered in solution and inactive in the binding assay.

Amino acid substitutions within the Asp-Lys-Trp core sequence of the 2F5 epitope adversely affect antibody reactivity resulting in a 10−100-fold loss in binding affinity (*9*, *10*). No single substitution could be tolerated that

maintained antibody affinity (*49*). Replacement of the Glu with an Asp residue at the $i + 4$ position (structure **4**) maintained the secondary structure and enhanced MAb affinity approximately 4-fold. The root-mean-square deviation (RMSD) of the ensemble of 31 NMR-derived structures of peptides **3** and **4** (backbone heavy atoms including the lactam bridge) was 1.28 versus 0.98 Å, respectively, consistent with the Asp substitution imparting greater backbone rigidity. All subsequent β-turn mimetics were synthesized with a lactam constraint incorporating an Asp residue in the $i + 4$ position.

Empirical data from our laboratories suggested that extensions of the 2F5 epitope increased the MAb 2F5 affinity (*29*). Structure **8** is an example of a linear N- and C-terminal extended 2F5-epitope sequence that demonstrates a significant enhancement in MAb 2F5 affinity although the peptide backbone is largely disordered in solution (data not shown). Relative to structure **4**, the doubly extended linear peptide is greater than 200-fold more potent in the MAb 2F5 affinity assay demonstrating that the 2F5 epitope is substantially longer than the previously identified 6-mer, Glu-Leu-Asp-Lys-Trp-Ala (*9*, *10*, *29*). This finding is consistent with the recently published findings of Parker et al., identifying the sequence, Asn-Glu-Gln-Glu-Leu-Leu-Glu-Leu-Asp-Lys-Trp-Ala-Ser-Leu-Trp-Asn, as the functional epitope recognized by MAb 2F5 (*50*).

Addition of a Glu-Leu-Leu segment to the N-terminus of structure **4** had a dramatic effect on MAb 2F5 binding (compare structures **4** and **9**) increasing affinity by 35-fold. Addition of the C-terminal segment Leu-Trp-Asn to structure **4** (structure **10**) enhanced affinity by 100-fold. Both peptides (structures **9** and **10**) adopt well-defined type I β-turns exhibiting modest affinity for MAb 2F5. On the basis of these findings, the combination of both N- and C-terminal amino acid extensions with the central lactam constraint (Dap to Asp, i to $i + 4$) should increase MAb 2F5 affinity while maintaining a reverse turn conformation. This is clearly demonstrated with peptide **6**, the most potent analogue of the series recognized by MAb 2F5. Qualitative analysis of the ROE data indicates that the peptide adopts a defined reverse turn centered about the Asp-Lys-Trp-Asp segment of the peptide backbone. The observation of moderate to strong intensity sequential amide NH ROEs between (1) Lys_7 and Trp_8 and (2) Trp_8 and Asp_9 are characteristic of a type I β-turn. The observed Asp_9 amide hydrogen temperature coefficient of -1.7 parts per billion (measured in DMSO-d_6) is consistent with an intramolecular hydrogen bond to the Asp_6 carbonyl oxygen.

Shown in Figure 2 is a GA-derived conformation of peptide **6** superimposed on the crystal structure of the antibody-bound 2F5 epitope (Glu-Leu-Asp-Lys-Trp-Ala-Ser). Peptide **6** adopts a well-defined, ideal type 1 β-turn centered about Asp-Trp-Lys-Asp (positions 1−4 of the turn). The N- and C-termini are disordered because of a paucity of experimentally observed ROEs, which is most likely due to flexibility of the termini in solution. The Lys side-chain resonances (β, γ, and δ protons) are shifted upfield in the proton spectrum by 0.4−0.8 ppm as compared to the random coil chemical shifts. This observation is consistent with crystallographic evidence of a cation/π-stacking interaction between the Lys_{665} and the Trp_{666} side chains in the antibody-bound epitope (*1*) (Figure 2).

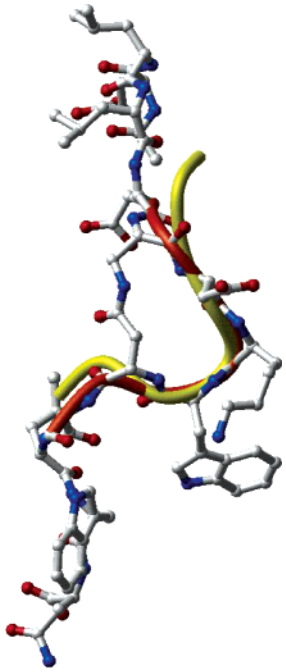

FIGURE 2: Superposition of structure **6** with the crystal structure of the 2F5 epitope. The NMR-derived solution structure of Ac-Glu_1-Leu_2-Leu_3-Glu_4-Dap_5-Asp_6-Lys_7-Trp_8-Ala_9-Ser_{10}-Leu_{11}-Trp_{12}-Asn_{13}-OH (cyclo(i to $i + 4$), Dap to Asp) is shown colored by atom type (hydrogen atoms are omitted for clarity). Shown in orange is only the Glu-Dap-Asp-Lys-Trp-Asp-Ser backbone segment of **6** illustrating the reverse turn conformation adopted by the peptide in solution. Shown in yellow is the crystal structure of the backbone atoms of the antibody-bound 2F5 epitope (Glu-Leu-Asp-Lys-Trp-Ala-Ser) (*1*). The dihedral angles that define the turn structure of **6** are as follows: ϕLys −29°, ψLys −67°, ϕTrp −119°, and ψTrp −16°. The dihedral angles defining the reverse turn for the crystal structure are as follows: ϕLys −50°, ψLys −36°, ϕTrp −104°, and ψTrp 11°. Sixty-five ROEs extracted from a ROESY spectrum recorded in PBS solution at 25 °C were included as distance constraints in the structural calculations. Two violations were identified: (1) Trp_8 H_4 to Trp_8 Hβ and (2) Trp_8 H_2 to Trp_8 Hβ. Both of these violations can be attributed to motional averaging of the Trp_8 indole ring. The Lys_7 ϕ angle was constrained to 60 ± 20° based on the observed vicinal coupling constant, $^3J_{HN\alpha}$, of 3.5 Hz. The Asp-Lys-Trp-Asp segment (positions 1−4) of the cyclic lactam adopts an ideal type I β-turn.

The concomitant use of DG with a GA enables one to rapidly determine which distance restraints will not be satisfied within a given structure. Following the elimination of any nonsatisfied distance constraints, conformations can then be generated using a traditional DG approach. Sixty-five distance constraints were extracted from a ROESY spectra recorded on structure **6** in PBS. The GA-derived conformation satisfied 63 constraints and was subsequently subjected to traditional distance geometry calculations to generate 100 conformations. This ensemble was subjected to energy minimization to quantitatively rank the energies of the individual structures (*48*, *51*). Conformations with energies greater than 20 kcal/mol above the global minimum energy were discarded resulting in 16 low energy conformations exhibiting energetically favorable torsion angles and van der Waals distances between nonbonded atoms. Fifteen of the 16 calculated structures adopt type I β-turns (eight type I, six nonideal type I, one type I′). The superposition of the backbone atoms of the Glu-Dap-Asp-Lys-Trp-Asp-Ser (Dap to Asp, cyclo(i to $i + 4$)) segment of the eight,

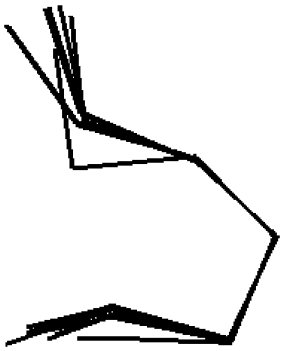

FIGURE 3: Superposition of the eight conformations of **6** exhibiting a type I β-turn. Superposition of the backbone atoms of the Glu-Dap-Asp-Lys-Trp-Asp-Ser (Dap to Asp, cyclo(i to $i + 4$)) segment of **6** (lactam bridge has been omitted for clarity). The backbone atom RMSD including the lactam constraint is 0.6 Å. The RMSD of the backbone heavy atoms comprising only the Asp-Lys-Trp segment is 0.06 Å.

ideal type I β-turns is depicted in Figure 3 (the lactam bridge has been omitted for clarity) (Figure 3).

A subsequent alanine scan study was performed on a segment of gp41 corresponding to residues 638−683 in the native sequence (*49*). The six residues within the 2F5 recognition epitope (Glu-Leu-Asp-Lys-Trp-Ala residues 662−667) and the 10 residues flanking the N- and C-termini of the epitope were individually replaced with an alanine. Individual substitution of either Asp_{664}, Lys_{665}, or Trp_{666} residues reduced the MAb 2F5 binding affinity by 2−3 orders of magnitude. Both Glu_{662} and Leu_{663} tolerate alanine substitution with negligible differences in binding affinity. Replacement of Ala_{667} by a Val had no effect on MAb 2F5 binding. Substitution of either Glu_{659} or Leu_{661} resulted in a 7-fold attenuation of antibody affinity indicating that both residues mediate specific interactions with MAb 2F5. These results demonstrate that noncontiguous residues N-terminal to the 2F5 epitope contribute to specific binding (Glu_{659} and Leu_{661}). Individual replacement of the 10 residues C-terminal to the epitope with alanines had no effect on MAb 2F5 affinity. The observed enhancement of MAb 2F5 affinity in the extended, constrained peptides (structures **9** and **10**) can be rationalized in light of the alanine scan results. The enhancement of MAb 2F5 affinity observed with the N-terminal extended structure (**9**) is consistent with the specific Glu_{659} and Leu_{661} contributions to MAb 2F5 binding observed in the alanine scan. The increased binding affinity observed with the C-terminal extended peptide (structure **10**) is most likely attributed to nonspecific binding effects or a synergistic interaction between multiple residues or both.

Peptides **11** and **12** were synthesized with a cysteine residue and a 6-aminohexanoic acid (Aha) spacer on either the amino- or the carboxyterminus for conjugation to a maleimide-activated carrier protein for animal immunization studies. The nonconjugated cyclic lactam macrocycle in both structures adopts a type I β-turn. The additional C- or N-terminal extension required for conjugation to the carrier protein does not perturb the overall conformation of the reverse turn or appreciably alter the antibody binding affinity.

Animal Immunization Studies. Groups of four guinea pigs were immunized three times with 100 μg of conjugate (prepared from peptides **11** and **12**) per animal at 4-week intervals. Three weeks following each immunization, serum samples were collected and tested for antibody titers against their corresponding free peptides as well as the linear, 13-residue 2F5 peptide (peptide **8**) (Table 2). Both conjugates elicited very high antibody titers to their respective free peptides. The antibody response exceeded a GMT of 1×10^6 titers at post-dose 2 and post-dose 3. A maximal antibody response is achieved after two immunizations. The serum samples were subsequently tested for HIV-1 neutralizing activity in a single cycle viral infectivity assay. Despite the high, peptide-specific antibody titers, the antisera failed to demonstrate any viral neutralizing activity. The structure of the conjugated immunogen may be important for immunogenicity but does not appear to be a prerequisite for the stimulation of a neutralizing antibody response (Table 2).

DISCUSSION

An effective, globally accessible therapy for the prevention or possible treatment of HIV-1 infection could come in the form of a vaccine. Ideally, a vaccine directed at HIV-1 would stimulate both a cell-mediated and humoral response, which is particularly important because of the high viral mutation rates. The design of an effective peptide immunogen capable of eliciting a broad-based immune response requires that an antigenic determinant be correctly presented in a specific three-dimensional structure. A segment of gp41, containing the previously identified MAb 2F5 epitope (Glu-Leu-Asp-Lys-Trp-Ala), is a viable target for the development of an HIV-1 vaccine. The 2F5 epitope is highly conserved and is capable of stimulating antibody that neutralize a wide array of HIV-1 viruses across different clades.

The focus of our work was to characterize the structural aspects of the 2F5 epitope responsible for recognition by MAb 2F5 and incorporate those features into a peptide immunogen construct capable of stimulating an effective immune response. The published crystal structure of the 2F5 epitope bound to the Fab fragment of MAb 2F5 revealed that the peptide adopts a well-defined, reverse turn conformation. Using a novel ELISA-based competition assay, structural features important for antibody avidity were identified from relative peptide−antibody affinities.

The crystal structure of the epitope−antibody complex revealed that the seven residue peptide (Glu-Leu-Asp-Lys-Trp-Ala-Ser) binds as a reverse turn with Asp-Lys-Trp-Ala comprising a type I β-turn. Initial attempts at constraining the peptides using an i to $i + 4$ lactam bridge resulted in well-defined reverse turn conformations in solution. Despite this fact, these peptides were only very weakly bound to the antibody, suggesting that the epitope was not in the correct conformation or additional regions beyond the defined 2F5 epitope may contribute to antibody affinity. Empirical data from our laboratories suggested that regions proximal to the defined 2F5 epitope are recognized by MAb 2F5 (*29*, *49*). These additional segments may stabilize the antibody-bound structure (*29*) or mediate specific interactions with the antibody. This observation was confirmed by extending the constrained peptides in both the N- and the C-terminal directions based on native gp41 sequence (structure **6**, Table 1). The extended peptide sequence, Ac-Glu-Leu-Leu-Glu-(Dap)-Asp-Lys-Trp-Asp-Ser-Leu-Trp-Asn-OH (Dap to Asp, i to $i + 4$ lactam bridge) displays the highest antibody affinity of the peptide immunogen series. Tian et al. (*52*) identified

Table 2: Induction of Antibody Response to 2F5 Peptides (Peptides **8**, **11**, and **12**) in Guinea Pigs

			Specific antibody titers									
			Postdose 1			Postdose 2			Postdose 3			postdose 3 neutralization[b]
vaccines	animals		**8**[a]	**11**[a]	**12**[a]	**8**[a]	**11**[a]	**12**[a]	**8**[a]	**11**[a]	**12**[a]	
11-OMPC[c]	1		25 600	102 400	409 600	1 638 400	6 553 600	6 553 600	1 638 400	6 553 600	1 638 400	<10
	2		25 600	102 400	102 400	1 638 400	6 553 600	4 634 095	1 638 400	1 638 400	1 638 400	<10
	3		25 600	409 600	409 600	1 638 400	6 553 600	6 553 600	1 638 400	6 553 600	1 638 400	<10
	4		102 400	1 638 400	1 638 400	1 638 400	6 553 600	6 553 600	1 638 400	6 553 600	1 638 400	<10
		GMT[d]	36 204	289 631	409 600	1 638 400	6 553 600	4 634 095	1 638 400	4 634 095	1 638 400	
OMPC-**12**[c]	1		102 400	102 400	409 600	1 638 400	1 638 400	6 553 600	6 553 600	1 638 400	1 638 400	<10
	2		102 400	409 600	409 600	1 638 400	6 553 600	6 553 600	6 553 600	1 638 400	1 638 400	<10
	3		102 400	409 600	409 600	6 553 600	6 553 600	6 553 600	1 638 400	1 638 400	6 553 600	<10
	4		409 600	409 600	409 600	6 553 600	6 553 600	6 553 600	6 553 600	6 553 600	6 553 600	<10
		GMT[d]	144 815	289 631	409 600	3 276 800	4 634 095	6 553 600	4 634 095	2 317 048	3 276 800	

[a] Three weeks following each immunization, post dose 1−3, serum samples were withdrawn, and antibody titers were determined. Peptide specific antibody titer levels were measured by an ELISA using native peptides **8**, **11**, and **12** immobilized on plastic. [b] HIV-1 infectivity inhibition data for guinea pig sera raised against peptides **8**, **11**, and **12**. Neutralization titers are defined as the reciprocal of the highest dilution giving 50% inhibition of infectivity. [c] Guinea pigs were immunized three times at four week intervals with either **11**-OMPC (C-terminal conjugated peptide) or OMPC-**12** (N-terminal conjugated peptide). [d] Data represent geometric mean titers (GMT) of four animals per group where the individual titers were defined as the dilution giving <2 times the optical density of the corresponding dilution of pre-bleed serum. The antibody titers were calculated as reciprocals of the highest dilutions, which gave optical density values above two standard deviations of the mean of the secondary antibody conjugate control.

the nonapeptide Leu-Glu-Leu-Asp-Lys-Trp-Ala-Ser-Leu as the epitope necessary for maximum antibody affinity. Furthermore, antibody-binding studies of disulfide-constrained analogues containing this sequence demonstrated that a 15 residue cyclic structure is required for optimal 2F5 affinity (*52*). These studies demonstrate that both the extension of the 2F5 epitope and a defined secondary structure (through the introduction of a chemical constraint) are necessary to maximize antibody binding.

The structure−activity relationships explored with the constrained peptide series identified several structural features critical for recognition by MAb 2F5. Incorporation of an *i* to *i* + 4 lactam bridge constrained the Asp-Lys-Trp-Glu segment of the 2F5 epitope into a defined reverse turn. Use of the *i* to *i* + 4 lactam bridge, as opposed to an *i* to *i* + 4 disulfide bond constraint, stabilizes the turn structure that enhances the binding to MAb 2F5 (compare structures **2** and **3**, Table 1). Furthermore, the direction and position of the amide bond within the lactam constraint (N- to C-terminal direction) is important for maintaining a predominate type I β-turn conformation. Decreasing the size of the macrocycle by the replacement of Glu_9 with an Asp (structure **3** vs structure **4**) increased the MAb 2F5 binding affinity. The enhanced antibody affinity is most likely due to increased rigidity of the smaller lactam macrocycle. Acetylation of the N-terminal Glu resulted in retention of MAb affinity. Since N-capping is an effective means of reducing proteolytic digestion of peptides, this chemical modification was incorporated into the subsequent immunogen constructs (compare structures **2** and **3**).

The OMPC-conjugated constrained peptides are highly immunogenic, raising high peptide-specific antibody titers in guinea pigs. Despite the high titers obtained, the immunogen constructs were incapable of stimulating a neutralizing response. There are a number of possible explanations for this finding. First, the conformation of the 2F5 recognition segment in the fusogenic state of the native virion is unknown. The results from our laboratory (*29*, *49*) redefined the 2F5 recognition sequence as a discontinuous epitope comprising the 13-residue segment, Glu-Leu-Leu-Glu-Leu-Asp-Lys-Trp-Ala-Ser-Leu-Trp-Asn. Parker et al. (*50*) and Tian et al. (*52*) have also identified extended, discontinuous epitopes. The extended epitopes may bind to the antibody in a conformation other than the reverse turn structure observed for Glu-Leu-Asp-Lys-Trp-Ala-Ser bound to MAb 2F5 in the crystal structure. Recent NMR and CD results from our laboratory have demonstrated that the C-terminal region of DP178 containing the 2F5 epitope adopts a defined helical conformation in an organic/water mixture (*49*). The linear peptide segment, Glu-Leu-Leu-Glu-Leu-Asp-Lys-Trp-Ala-Ser-Leu-Trp-Asn, corresponding to residues 659−671 of the gp41 ectodomain has been shown to adopt a 3(10)-helix in water (*53*). The helical propensity observed for the C-terminal region of DP178 may reflect the conformation in the native virion. Additional crystallographic or NMR studies of the extended epitope bound to MAb 2F5 are necessary to address this unresolved issue.

Second, the structure of the peptides following conjugation to OMPC is not known. Despite the presence of a predominate reverse turn conformation adopted by the nonconjugated constrained constructs in solution, cyclic peptides are inherently flexible. Conjugation may in fact perturb the reverse turn structure presenting the epitope in a biologically nonrelevant conformation. Conjugation to carrier proteins may pose additional problems; the conjugate may be unstable, or alteration of the peptide moieties following conjugation can occur (*54*). The high titers induced by the conjugated constrained peptides indicate that these peptides are highly immunogenic; however, this conformation may not be a requirement for the stimulation of a neutralizing response (Table 2). Given the existing data, it is not possible to determine if the conformation of the constrained peptide is altered following conjugation or if the reverse turn is maintained but is biologically irrelevant in regard to eliciting a neutralizing response. The conserved segment, Glu-Leu-Asp-Lys-Trp-Ala, has been inserted into both the *Escherichia coli* MalE-hybrid proteins and the antigenic site B of the influenza virus hemagglutinin; in both cases, a humoral, nonneutralizing immune response was elicited against HIV-1 (*55*, *56*).

Third, approximately 50% of HIV-1 infected humans have a detectable antibody response to the 2F5 epitope on gp41 (*10*, *57*). However, generation of a broadly neutralizing antibody response solely targeted to the 2F5 epitope is a relatively rare event during natural infection (*10*). Among serum antibodies recognizing the 2F5 epitope, those that have neutralizing potential may be at concentrations insufficient to block HIV-1 infection in cell culture. A high titer polyclonal response containing insufficient concentrations and/or low affinity neutralizing antibodies is essentially indistinguishable from a nonneutralizing effect. Therefore, HIV-1 neutralization would only occur at antibody concentrations significantly higher than seen in a typical immune response that is characterized by high affinity antibodies at low to moderate concentrations. Conversely, neutralization of HIV-1 may only occur with antibody binding to more than one site; thus, a 2F5 mediated response alone may not be sufficient (*57*). Furthermore, the human 2F5 antibody has a significantly longer complementarity determining region (CDR3) loop (*58*) that may account for the rare 2F5 occurrence in infected sera. The CDR3 loop is much shorter in guinea pigs, and as a consequence, a 2F5-like response may not be possible in rodents but still may be observed in humans.

Last, binding of the 2F5 epitope alone is insufficient for blocking entry. The 2F5 MAb may make additional membrane or protein contacts through the long CDR3 loop, which are not observed in the crystal structure. If so, it maybe impossible to elicit antibodies such as 2F5 with immunogens comprising only the core peptide epitope. Additional studies are necessary to fully exploit the immunological properties of the 2F5 epitope toward the development of an efficacious HIV-1 vaccine.

ACKNOWLEDGMENT

The authors acknowledge the valuable scientific contributions of Drs. A. Pessi and E. Bianchi to the gp41 vaccine project. The authors (G.B.M.) thank Drs. J. C. Culberson and S. K. Kearsley for useful discussions pertaining to the distance geometry algorithm. We also wish to thank Drs. H. G. Ramjit and C. W. Ross, III for the exact mass measurements and Ms. J. Williams for the preparation of Figure 1 and Table 1. We thank Dr. S. Pitzenberger for a critical reading of the manuscript, and we thank Ms. C. Wu for the synthesis of structure **8**.

REFERENCES

1. Pai, E. F., Klein, M. H., Chong, P., Pedyczak, A. (2000) World Intellectual Property Organization Patent WO-00/61618.
2. Chan, D. C., and Kim, P. S. (1998) *Retroviruses Hum. AIDS Relat. Anim. Dis., Colloq. Cent Gardes*, 11th Meeting Date 1997, 105−111.
3. Freed, E. O., and Martin, M. A. (1995) *J. Biol. Chem. 270*, 23883−23886.
4. Luciw, P. A. (1996) Human Immunodeficieny Virus and Their Replication, in *Fields Virology* (Fields, B. N., Knipe, D. W., Howley, P. M. et al., Eds.) 3rd ed., pp 1881−1952, Lippincott-Raven Publishers, Philadelphia.
5. Broder, C. C., and Dimitrov, D. S. (1996) *Pathobiology 64*, 171−179.
6. D'Souza, M. P., and Harden, V. A. (1996) *Nat. Med. 2*, 1293−1300.
7. Wilkinson, D. (1996) *Curr. Biol. 6*, 1051−1053.
8. Chan, D. C., Fass, D., Berger, J. M., and Kim, P. S. (1997) *Cell 89*, 263−273.
9. Muster, T., Steindl, F., Purtscher, M., Trkola, A., Klima, A., Himmler, G., Rüker, F., and Katinger, H. (1993) *J. Virol. 67*, 6642−6647.
10. Conley, A. J., Kessler, J. A., II, Boots, L. J., Tung, J.-S., Arnold, B. A., Keller, P. M., Shaw, A. R., and Emini, E. A (1994) *PNAS 91*, 3348−3352.
11. Salzwedel, K., West, J. T., and Hunter, E. (1999) *J. Virol. 73*, 2469−2480.
12. Suárez, T., Gallaher, W. R., Agirre, A., Goñi, F. M., and Nieva, J. L. (2000) *J. Virol. 74*, 8038−8047.
13. Schibli, D. J., Montelaro, R. C., and Vogel, H. J. (2001) *Biochemistry 40*, 9570−9578.
14. Chan, D. C., and Kim, P. S. (1998) *Cell 93*, 681−684.
15. Root, M. J., Kay, M. S., and Kim, P. S. (2001) *Science 291*, 884−888.
16. Wild, C. T., Shugars, D. C., Greenwell, T. K., McDanal, C. B., and Matthews, T. J. (1994) *PNAS 91*, 9770−9774.
17. Judice, J. K., Tom, J. Y. K., Huang, W., Wrin, T., Vennari, J., Petropoulos, C. J., and McDowell, R. S. (1997) *PNAS 94*, 13426−13430.
18. Jiang, S., Lin, K., Strick, N., and Neurath, A. R. (1993) *Nature 365*, 113.
19. Lawless, M. K., Barney, S., Guthrie, K. I., Bucy, T. B., Petteway, S. R., and Merutka, G. (1996) *Biochemistry 35*, 13697−13708.
20. Kilby, J. M., Hopkins, S., Venetta, T. M., DiMassimo, B., Cloud, G. A., Lee, J. Y., Alldredge, L., Hunter, E., Lambert, D., Bolognesi, D., Matthews, T., Johnson, M. R., Nowak, M. A., Shaw, G. M., and Saag, M. S. (1998) *Nat. Med. 4*, 1302−1307.
21. Richman, D. D. (1998) *Nat. Med. 4*, 1232−1233.
22. Klein, M. (2001) *Vaccine 19*, 2210−2215.
23. Burton, D. R. (1997) *PNAS 94*, 10018−10023.
24. Stiegler, G., Kunert, R., Purtscher, M., Wolbank, S., Voglauer, R., Steindl, F., and Katinger, H. (2001) *AIDS Res. Hum. Retroviruses 17*, 1757−1765.
25. Zwick, M. N., Labrijn, A. F., Wang, M., Spenlehauer, C., Saphire, E. O., Binley, J. M., Morre, J. P., Stiegler, G., Katinger, H., Burton, D. R., and Parren, P. W. (2001) *J. Virol. 75*, 10892−18905.
26. Zwick, M. B., Bonnycastle, L. L. C., Menendez, A., Irving, M. B., Barbas, C. F., Parren, P. W. H. I., and Burton, D. R. (2001) *J. Virol. 75*, 6692−6699.
27. Trkola, A., Purtscher, M., Muster, T., Ballaun, C., Buchacher, A., Sullivan, N., Srinivasan, K., Sodroski, J., Moore, J. P., and Katinger, H. (1996) *J. Virol. 70*, 1100−1108.
28. Moulard, M., Phogat, S. K., Shu, Y., Labrijn, A. F., Xiao, X., Binley, J. M., Zhang, M. Y., Sidorov, I. A., Broder, C. C., Robinson, J., Parren, P. W., Burton, D. R., and Dimitrov, D. S. (2002) *PNAS 10*, 6913−1918.
29. Barbato, G. et al., personal communications.
30. Merrifield, R. B. (1964) *Biochemistry 3*, 1385−1390.
31. Felix, A. M., Heimer, E. P., Wang, C.-T., Lambros, T. J., Fournier, A., Mowles, T. F., Maines, S., Campbell, R. M., Wegrzynski, B. B., Toome, V., Fry, D., and Madison, V. S. (1988) *Int. J. Pept. Protein Res. 32*, 441−454.
32. Frasch, C. E., and Robbins, J. D. (1978) *J. Exp. Med. 147*, 629−644.
33. Marburg, S., Jorn, D., Tolman, R. L., Arison, B., McCauley, J., Kniskern, P. J., Hagopian, A., and Vella, P. P. (1986) *J. Am. Chem. Soc. 108*, 5282−5287.
34. Ellman, G. L. (1959) *Arch. Biochem. Biophys. 82*, 70−77.
35. Markwell, M. A., Haas, S. M., Bieber, L. L., and Tolbert, N. E. (1978) *Anal. Biochem. 87*, 206−210.
36. Shuler, K. R., Dunham, R. G., and Kanda, P. (1992) *J. Immunol. Methods 156*, 137−149.
37. Charneau, P. M., Alizon, M., and Clavel, F. (1992) *J. Virol. 66*, 2814−20.
38. Braunschweiler, L., and Ernst, R. R. (1983) *J. Magn. Reson. 55*, 521−526.
39. Bax, A., and Davis, D. G. (1985) *J. Magn. Reson. 65*, 355−360.
40. Bothner-By, A. A., Stephens, R. L., Lee, J., Warren, C. D., and Jean-loz, R. W. (1984*) J. Am. Chem. Soc. 106*, 811−813.
41. Bax, A., and Davis, D. D. (1985) *J. Magn. Reson. 63*, 207−213.
42. Levitt, M. H., Freeman, R., and Frenkiel, T. (1982) *J. Magn. Reson. 47*, 328−330.
43. Cavanagh, J., and Keeler, J. (1988) *J. Magn. Reson. 80*, 186−194.
44. Griesinger, C., and Ernst, R. R. (1987) *J. Magn. Reson. 75*, 261−271.
45. Thomas, P. D., Basus, V. J., and James, T. L. (1991) *Proc. Natl. Acad. Sci U.S.A. 88*, 1237−1241.

46. Kearsley, S., personal communication (unpublished Distance Geometry/Genetic Algorithm code developed in-house).
47. Ma, J. C., and Dougherty, D. A. (1997) *Chem. Rev. 97*, 1303−1324.
48. Halgren, T. A. (1999) *J. Comput. Chem. 20*, 720−729.
49. Joyce, J. G., Hurni, W. M., Bogusky, M. J., Garsky, V. M., Liang, X., Citron, M. P., Danzeisen, R. C., Miller, M. D., Shiver, J. W., and Keller, P. M. (2002) *J. Biol. Chem. 277*, 45811−45820.
50. Parker, C. E., Deterding, L. J., Hager-Braun, C., Binley, J. M., Schülke, N., Katinger, H., Moore, J. P., and Tomer, K. (2001) *J. Virol. 75*, 10906−10911.
51. Mohamadi, F., Richards, N. G. J., Guida, W. C., Liskamp, R., Lipton, M., Caufield, C., Chang, G., Hendrickson, T., and Still, W. C. (1990) *J. Comput. Chem. 11*, 440.
52. Tian, Y., Ramesh, C. V., Ma, X., Naqvi, S., Patel, T., Cenizal, T., Tiscione, M., Diaz, K., Crea, T., Arnold, E., Arnold, G. F., and Taylor, J. W. (2002) *J. Pept. Res. 59*, 264−276.
53. Biron, Z., Zhare, S., Samson, A. O., Hayek, Y., Naider, F., and Anglister, J. (2002) *Biochemistry 41*, 12687−12696.
54. Briand, J. P., Muller, S., and van Regenmortel, M. H. V. (1985) *J. Immunol. Methods 173*, 59−69.
55. Coëffier, E., Clément, J.-M., Cussac, V., Khodaei-Boorane, N., Jehanno, M., Rojas, M., Dridi, A., Latour, M., El Habib, R., Barré-Sinoussi, F., Hofnung, M., and Leclerc, C. (2001) *Vaccine 19*, 684−693.
56. Muster, T., Ferko, B., Klima, A., Purtscher, M., Schulz, P., Grassauer, A., Katinger, H., Engelhardt, O., Garcia-Sastre, A., and Palese, P. Secretory Antibodies Against HIV-1 Induced by a Chimeric Influenza Virus, in *Vaccines 95: Molecular Approaches to the Control of Infectious Diseases* (Chanock, R., Ed.) pp 363−368, Cold Spring Harbor Laboratory Press, Plainview, NY.
57. Broliden, P.-A., von Gegerfelt, A., Clapham, P., Rosen, J., Fenyö, E.-M., Wahren, B., and Broliden, K. (1992) *Proc. Natl. Acad. Sci. U.S.A. 89*, 461−465.
58. Kunert, R., Ruker, F., and Katinger, H. (1998) *AIDS Res. Hum. Retrovir. 14*, 1115−1128.

BI026952U